



Influence of interlayer cations on the water sorption and swelling–shrinkage of MX80 bentonite

G. Montes-H^{a,*}, J. Duplay^a, L. Martinez^b, Y. Geraud^a, B. Rousset-Tournier^a

^aUMR 7517 ULP-CNRS, CGS 1, rue Blessig, Strasbourg F-67084, France

^bUMR G2R/7566, UHP Nancy 1, BP 239, Vandoeuvre Cedex 54506, France

Received 24 July 2002; accepted 16 April 2003

Abstract

The potential of water sorption and swelling–shrinkage in the expansive clays is practically defined by the nature of interlayer cations. The purpose of this paper is to estimate the effects of the cation saturation (Mg^{2+} , Ca^{2+} , Li^{+} , Na^{+} , and K^{+}) on the swelling–shrinkage behaviour of the MX80 bentonite.

The MX80 bentonite (a “commercial clay”) was treated with concentrated solutions (1 N) of sodium, calcium, magnesium, potassium, and lithium chlorides. This treatment was made three times with constant agitation for 1 h. Then, the clay was washed three times with distilled water. The scanning transmission electron microscopy (STEM) and inductively coupled plasma atomic emission microscopy (ICP-AES) analyses were used to verify the efficiency of the cation saturation.

Finally, two techniques were employed to estimate the effect of the cation saturation on the swelling–shrinkage behaviour of the bentonite: the first one uses an isothermal system of water adsorption, where the water activity is controlled by a supersaturated salt solution. In the second, environmental scanning electron microscopy (ESEM), coupled with a digital image analysis (DIA) program, was used to estimate the swelling–shrinkage potential at different water activities. The swelling–shrinkage isotherms were always estimated on isolated aggregates.

The isotherms of water adsorption and swelling–shrinkage of the bentonite MX80 show that the amount of adsorbed water and the swelling–shrinkage potential depend directly on the interlayer cation. For example, the sodium bentonite presents an excellent capacity to swell while the lithium bentonite does not swell significantly at the aggregate scale. In addition, other textural properties may be modified by the cation saturation, such as the specific surface, the particle size, porosity, etc.

© 2003 Elsevier B.V. All rights reserved.

Keywords: Swelling–shrinkage; Interlayer cations; Bentonite; ESEM; Digital image analysis

1. Introduction

Knowing how much water is taken up by clay is basic for many applications and also helps to charac-

terize a clay, but it is important to make the measurements under well-defined conditions (of ambient temperature and of relative humidity). If, in addition, the equilibrium amount of water sorbed is measured as a function of water vapor pressure under isothermal conditions, the sorption isotherm so determined can be analysed further to make deductions about the extent of the clay surface and the free energy of its interaction with water (Velde, 1992; Newman, 1987).

* Corresponding author. Fax: +33-38-8367235.

E-mail addresses: montes@illite.u-strasbg.fr, german_montes@hotmail.com (G. Montes-H).

For many layer silicates in which isomorphous ion replacement causes a net deficit of positive charge within the sheet, the deficit is balanced by interlayer cations. In a natural medium, the balancing cations can be accessible from the surrounding medium, and if this is an aqueous salt solution, the cation can exchange for other cations. Under these conditions, double layers develop, whose nature and thickness depend on the balancing cation, on the surface density of charge, and on the concentration of the salt solution (Newman, 1987; Kinuthia et al., 1999).

In general, the 2:1 minerals group, comprising vermiculites and smectites including montmorillonite, beidellite, hectorite, saponite, and other varieties, have many features in common in their interaction with water. As they all contain a large proportion of swelling interlayers in which the water is arranged in a partly ordered structure around the interlayer cations, the cations themselves play a dominant role in their interaction with water. Not only does the interlamellar spacing depend on the cation, but also do the absolute amounts of sorbed water, the shape of the sorption isotherm, and the acidity function of the water. All these properties are influenced by the cation size, its valency, its electronegativity, and its hydration energy. For example, when dry montmorillonite is placed in a moist atmosphere, it is able to take up water vapour by adsorbing it in the interlayer region. Swelling leads to the moving apart or disjoining of the clay particles, especially those in a parallel arrangement, until they reach their equilibrium separation under a given pressure. The increase in the *c*-spacing, or the degree of expansion of the layers planes, depends on the cations located in the interlayer region. If the interlayer cations are monovalent and strongly hydrated (Na^+ and Li^+), the interplatelet repulsion is stronger and the degree of platelet separation is larger (Luckham and Rossi, 1999; Velde, 1992; Newman, 1987; Kinuthia et al., 1999).

The main aim of the current study has been to estimate the influence of interlayer cation in water sorption and swelling–shrinkage of the MX80 bentonite. For this purpose, two analytical techniques were performed. The first, isothermal sorption, was used to estimate the sorption isotherm for each bentonite exchanged sample (Na, Li, Mg, Ca, and K). The second used environmental scanning electron microscopy (ESEM), coupled with a digital image analysis

(DIA) program, to estimate the swelling–shrinkage isotherm on the same bentonite or isolated aggregate of exchanged sample.

Microscopic observations of hydrated samples were made possible by a recent tool, the environmental microscope (ESEM). Its great advantage is its ability to maintain the samples in hydrated states and to change the relative humidity in the sample surrounding. Experiments were performed to observe the swelling–shrinkage at different water activities of “bentonite–isolated aggregates.” The aggregate swelling–shrinkage quantification was achieved using a digital image analysis program (Visilog 5.3). This digital image analysis consists of a “bidimensional estimation (2D)” of an aggregate swelled at different water activities.

2. Experimental methods

2.1. MX80 bentonite composition

Several analytical methods were performed by different French laboratories to estimate the mineral composition of MX80 bentonite. This industrial bentonite contains about 80% of a low-charge montmorillonite with mixed “Na–Ca” filling interlayer. The accessory minerals and their proportions are shown Table 1.

Table 1
Mineral composition of the MX80 bentonite

	Proportion (%)	Proportion (%) “without molecular water” drying at 105 °C
Montmorillonite	70.6 ± 2.7	79.2 ± 3.0
Phlogopite (1 M)	2.7 ± 2.7	3.0 ± 3.0
Pyrite	0.5	0.6
Calcite	0.7 ± 0.5	0.8 ± 0.6
Ankérítite	1.0 ± 0.3	1.1 ± 0.4
Anatase	0.1	0.1
Plagioclases	8.2 ± 2.7	9.2 ± 3.0
Feldspath K	1.8 ± 1.8	2.0 ± 2.0
Phosphate	0.6	0.6
Quartz + cristobalite	2.5 ± 2.5	2.8 ± 2.8
Fe ₂ O ₃	0.4 ± 0.3	0.5 ± 0.4
Molecular water	10.8	–
Organic carbon	0.1	0.1
Total	100	100

ICP-MS and other complementary analysis (Sauzeat et al., 2001).

2.2. Cation saturation

To determine the effect of exchanged cation, the bulk samples of MX80 bentonite were treated separately with five concentrated solutions (1 N concentration) of sodium, lithium, calcium, magnesium, and potassium chlorides. All salts have the same ionic force ($I=2$).

Twenty grams of MX80 bentonite was dispersed into 1 l of salt solution (1 N) at 60 °C. This suspension was vigorously stirred with magnetic agitation for 1 h at 60 °C. Then, the cation-saturated clay was separated by centrifugation (15 min at 13,000 rpm) and decantation of the supernatant solutions. This process was repeated three times. The cation-saturated bentonite was then washed three to four times with distilled water until the AgNO_3 test for chloride became negative (Lee and Kim, 2002; Rytwo, 1996).

The cation-saturated bentonite was subsequently dried for 48 h at 60 °C and finally ground for 2 min (Touret, 1988).

2.3. Isothermal water sorption

Adsorption/desorption isotherms of water vapour at 23 °C were obtained using plastic desiccators (2 l) containing 1 g of sample (cation-saturated bentonite) previously dried for 24 h at 110 °C. Water activity was controlled with oversaturated salt solutions. These solutions were used to keep constant water activity of air in the plastic desiccators and surrounding sample contained in the glass jar.

The desiccators were kept in a constant room temperature (23 °C). Weighing was done every 3 days by a digital balance (accuracy=0.0001 g) until apparent equilibrium was reached (Rousset-Tournier, 2001).

2.3.1. Water content

The amount of adsorbed water in a sample after equilibration time was calculated using the following formula:

$$W = \frac{w_e - w_s}{w_s} \quad (1)$$

where w_e represents the weight of the humid sample at equilibrium (g) and w_s represents the weight of the dry sample (g).

2.3.2. Measurements accuracy

This essentially depends on the instrument quality (balance and thermal regulation system) and also on the attention taken during weighing. Here only the weighing accuracy was considered. The absolute error on the amount of adsorbed water was calculated using the following formula:

$$\Delta W = \frac{\Delta w}{w_s} (2 + W) \quad (2)$$

where Δw is the balance accuracy (0.0001 g).

2.3.3. Experimental data fitting

Experimental water adsorption data were fitted by the D'Arcy and Watt equation. This equation considers the monolayer (Langmuir) and multilayer (BET) adsorption (Sychev et al., 2001). The equation used in terms of water activity a_w was:

$$W = \frac{w_1 c_1 a_w}{1 + c_1 a_w} + p a_w + \frac{w_M c_M a_w}{1 - c_M} \quad (3)$$

where W is the amount of water adsorbed; w_1 and w_M are the densities of the primary and multilayer adsorption sites, respectively; c_1 and c_M are the interaction parameters related to the heat of adsorption on the primary adsorption sites and in the multilayer, respectively; and p is a constant included in the linear form of the adsorption isotherm.

A computer program (SigmaPlot2000) based on the nonlinear least squares analysis was used for fitting the equation to the water adsorption data. This fitting was only used to characterize the shape of adsorption–desorption isotherms.

2.4. ESEM methodology

For all environmental scanning electron microscope investigations, an XL30 ESEM LaB6 (FEI and Philips), fitted with a gaseous secondary electron detector (GSED) to produce a surface image, was used. This microscope is also equipped with a “cooling stage” to control the sample temperature.

Each sample was submitted to a hydration and then, respectively, dehydration cycle, with progressively increasing and decreasing water activity. This

Table 2
Pressures used to control the constant water activity in the ESEM chamber

Constant temperature of sample = 9 °C			
	Chamber Pressure (Torr)	Water activity a_w	
Swelling ● ↓	2.6	0.3	Shrinkage ↑ ●
	3.4	0.4	
	4.3	0.5	
	5.2	0.6	
	6.0	0.7	
	6.4	0.75	
	6.9	0.80	

process, coupled with the digital image analysis, was used to estimate the swelling–shrinkage isotherm for each cation-saturated bentonite (Montes-H, 2002).

ESEM manipulation to study the swelling–shrinkage potential consists basically of three stages.

2.4.1. Drying

The chamber pressure and sample temperature are, respectively, fixed at 2.3 Torr and 50 °C. This condition comprises a water activity of 0.025 on the sample according to the water phases diagram. The sample was kept under these “reference conditions” for about 15 min, and an image of an aggregate of interest was chosen and stored in the hard disk of the control PC.

2.4.2. Swelling

This manipulation was achieved at a constant sample temperature of 9 °C. Then the progressive sample hydration was performed by increasing the chamber pressure until water oversaturation of the

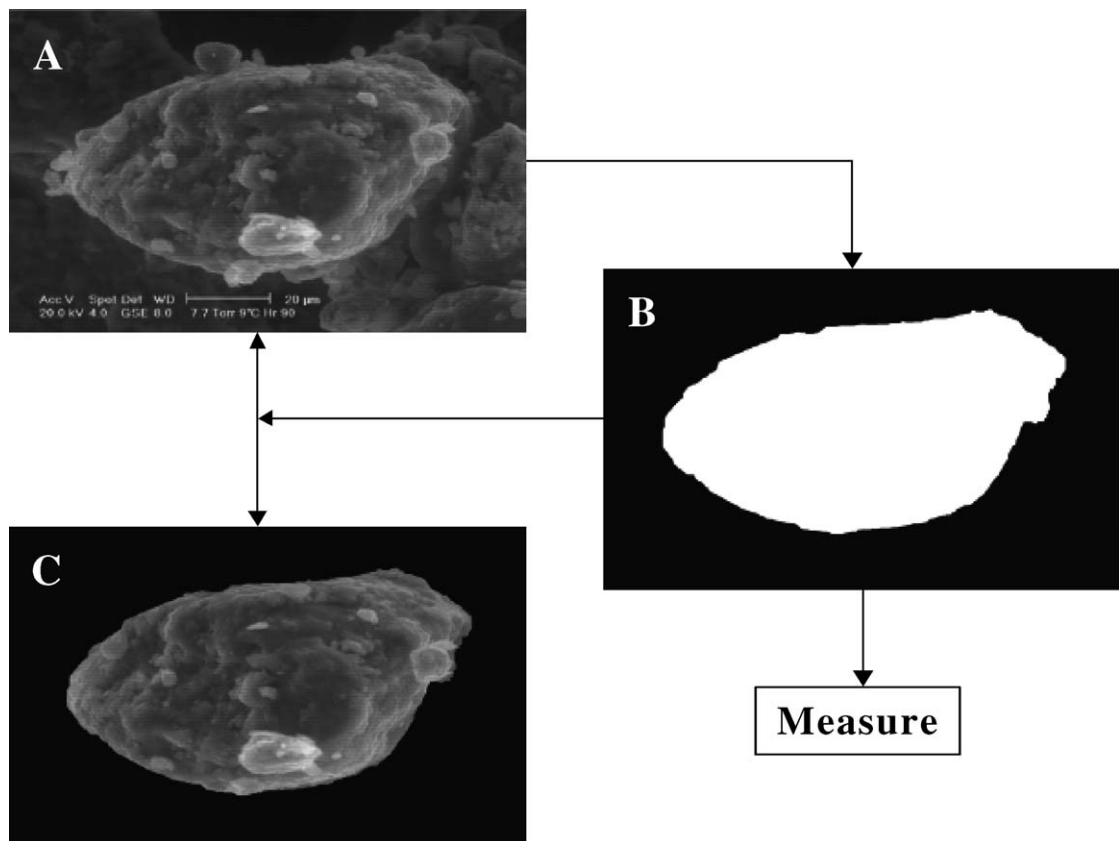


Fig. 1. Digital image analysis methodology. (A) ESEM image. (B) Image binarization and isolation of the surface “aggregate” of interest. (C) Image reconstitution and control verification.

sample was achieved. In all cases, the water oversaturation was observed at 0.8 water activity.

The pressures shown in Table 2 were used to keep a constant water activity of air in the ESEM chamber and the surrounding sample. In each step of chamber pressure, an image of interest was taken after 5 min.

This time was considered as equilibrium time and was previously estimated by kinetic manipulations.

2.4.3. Shrinkage

This stage was done inversely to that of swelling. Here the chamber pressure was progressively

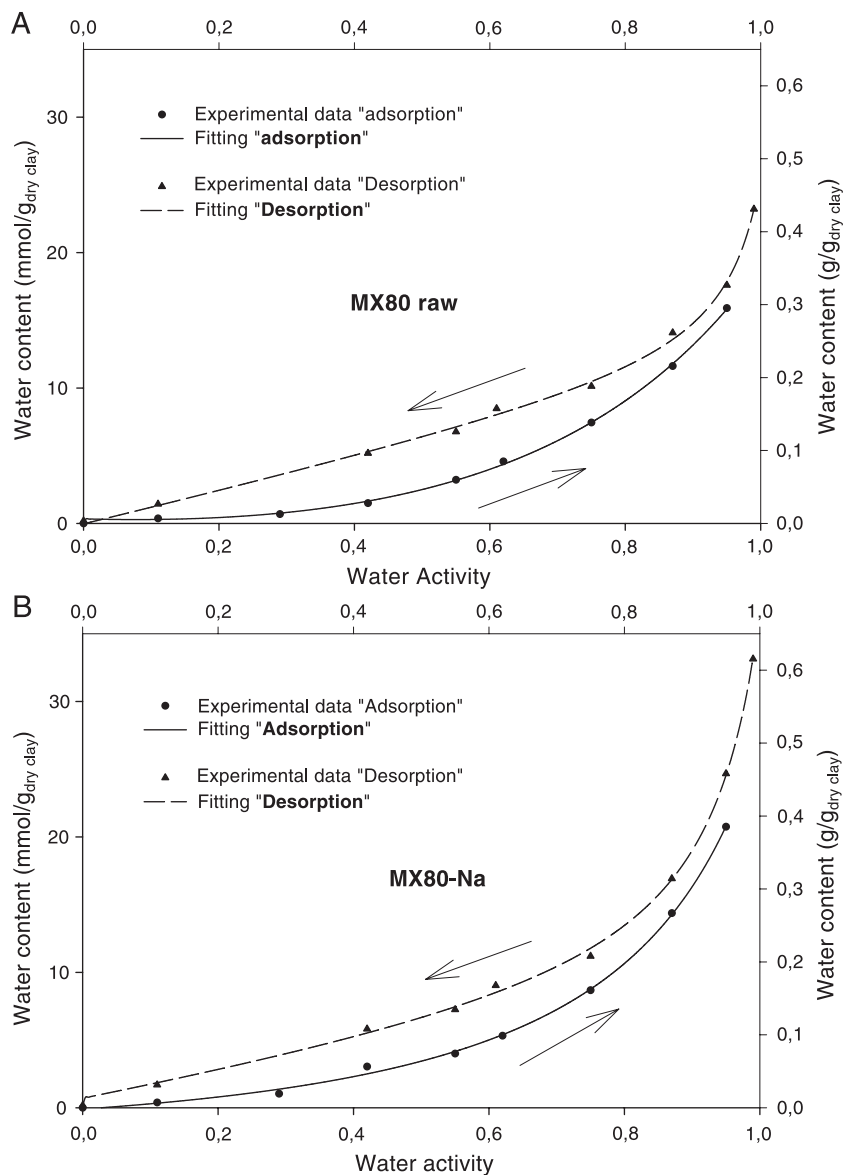


Fig. 2. Experimental adsorption–desorption isotherms and fitting by the D’Arcy–Watt equation. (A) Natural bentonite “MX80 raw.” (B) Na-saturated bentonite “MX80–Na.” (C) Li-saturated bentonite “MX80–Li.” (D) Ca-saturated bentonite “MX80–Ca.” (E) Mg-saturated bentonite “MX80–Mg.” (F) K-saturated bentonite “MX80–K.”

decreased until the reference conditions had been achieved (see Table 2). The sample temperature was always kept at 9 °C.

2.4.3.1. Swelling–shrinkage potential. The swelling–shrinkage potential was estimated by digital image analysis “bidimensional analysis” where the swelling–shrinkage potential in a sample after equili-

bration time was calculated from the following formula:

$$S = \frac{S_e - S_i}{S_i} 100 \quad (4)$$

where S_e represents the surface area of the humid sample (aggregate) at equilibrium (μm^2) and S_i represents the initial surface area of the dry sample (μm^2).

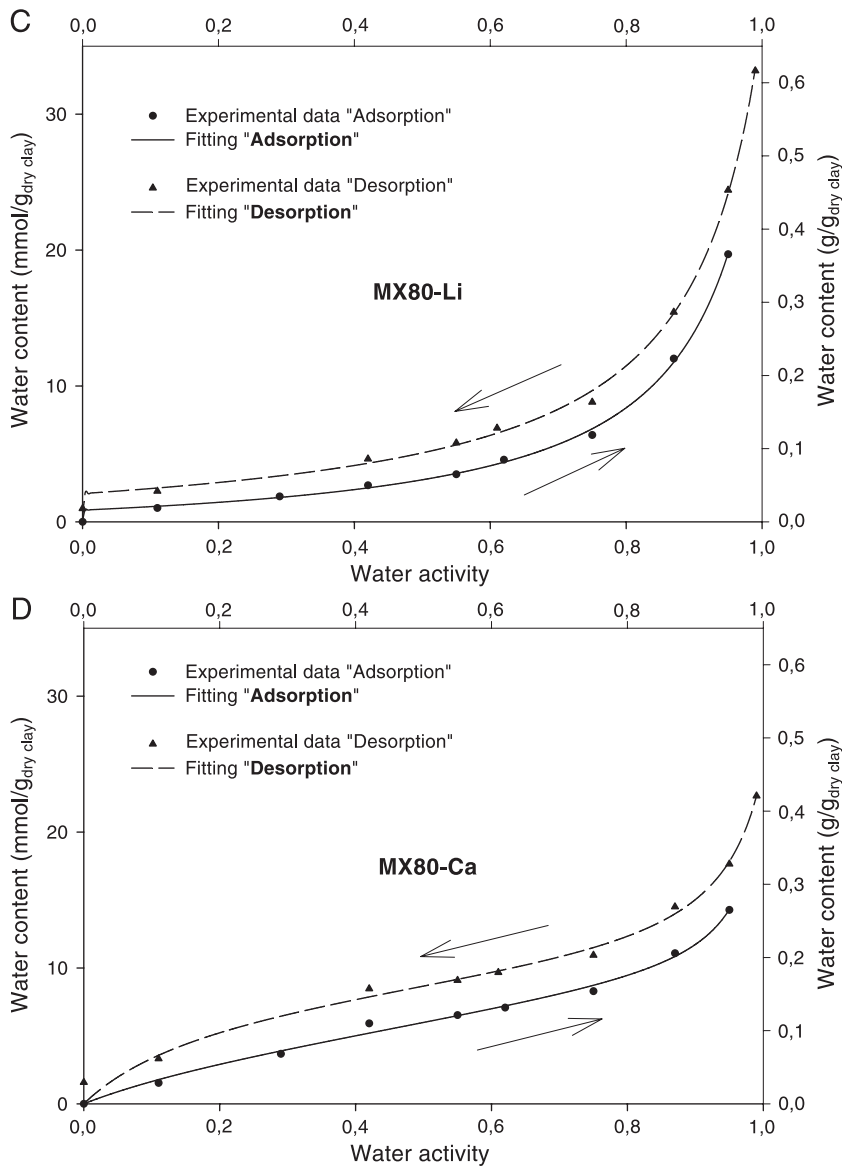


Fig. 2 (continued).

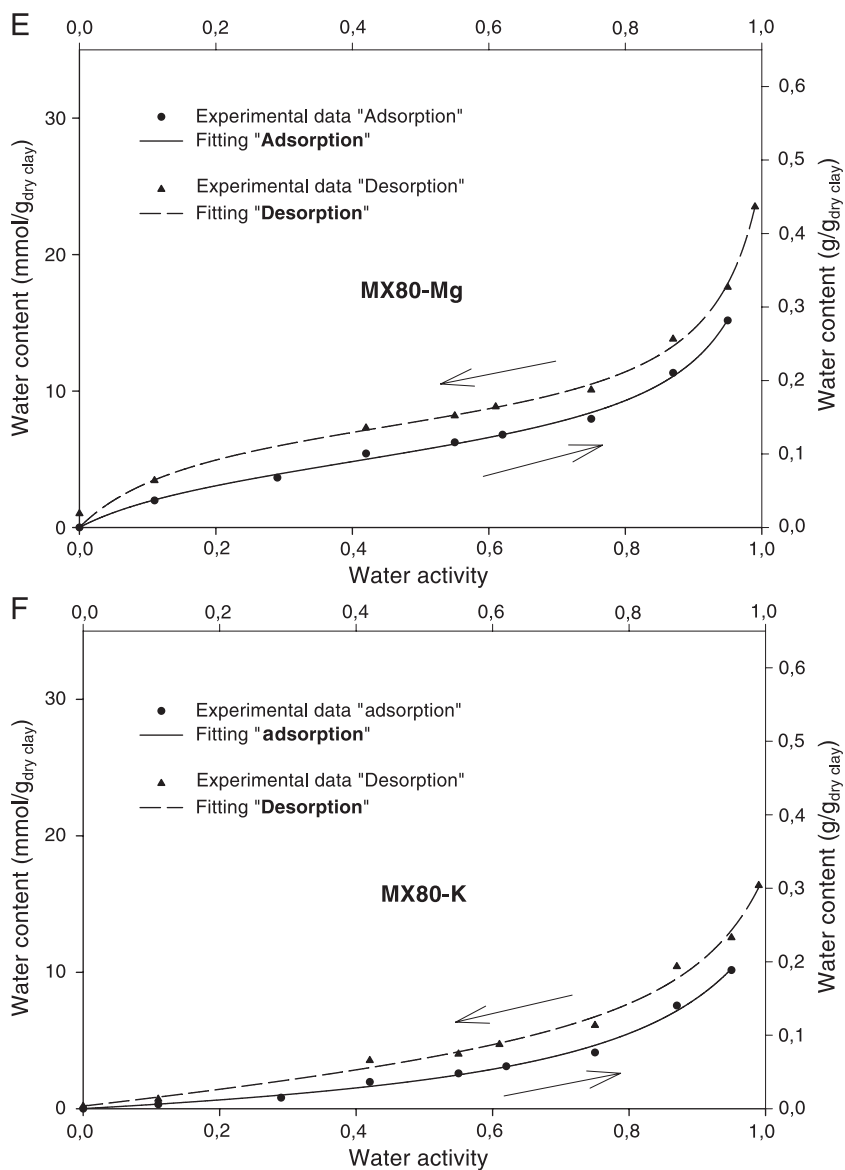


Fig. 2 (continued).

2.4.3.2. *Measurements accuracy.* The average standard deviation obtained after five repeated surface measurements was considered as an estimate of the absolute error on swelling–shrinkage:

$$E = \frac{s(\bar{q})}{S_i} (200 + S) \quad (5)$$

where $s(\bar{q})$ is the average standard deviation, S_i is the initial surface, and S is the swelling–shrinkage potential.

2.5. DIA methodology

Digital image analysis consists of isolating an area of interest by a commercial software (Visilog 5.3). In

this study, the area of interest was always an aggregate.

Generally, the ESEM images have sufficient density contrast to isolate the area of interest by applying a simple gray level threshold. To minimize the experimental error of the surface measure, the same procedure (i.e., the digital image analysis) was applied

manually five times. In addition, each analysis was visually controlled by the reconstitution of a binary image (Fig. 1).

The ESEM images of the test section occupied about 1424×968 pixels, and in all measurements, the same gray level range “0–256” has been considered.

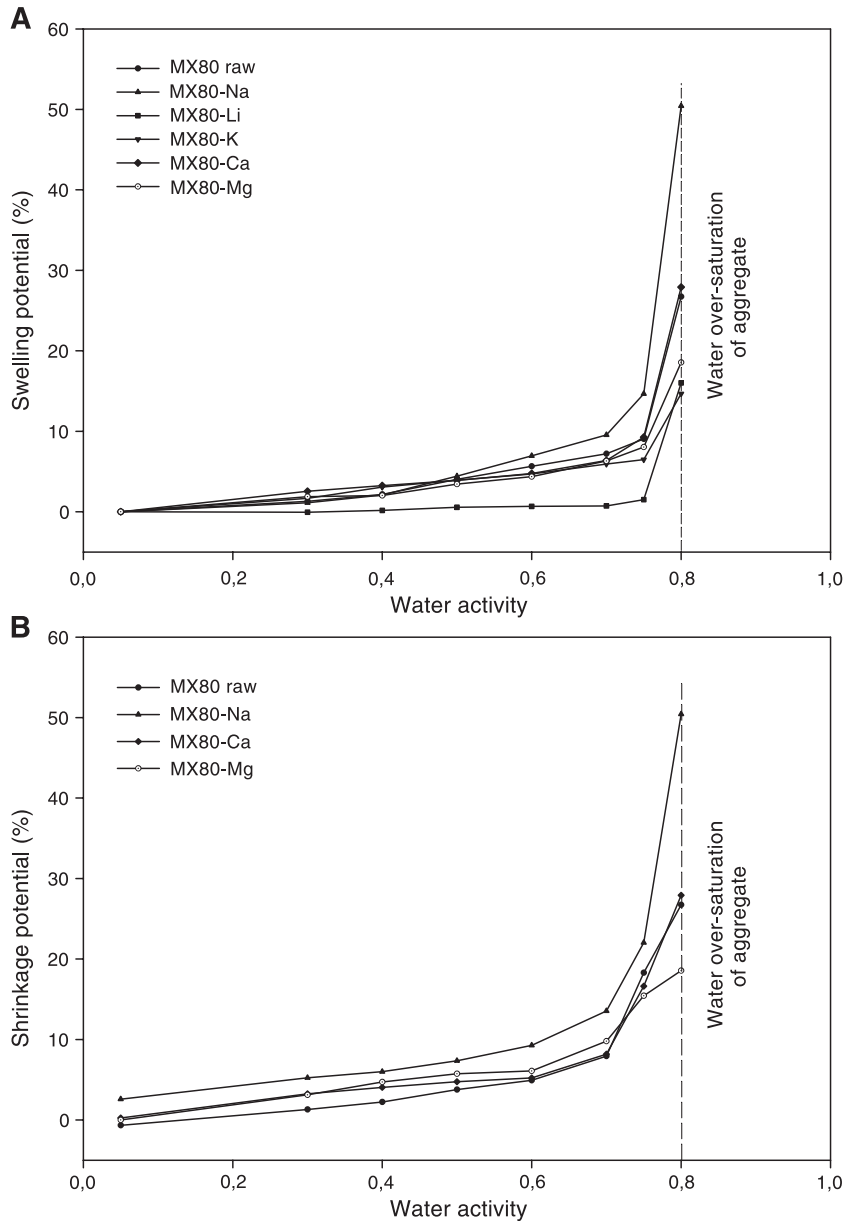


Fig. 3. Cation-saturated and natural bentonites isotherms by ESEM-DIA. (A) Swelling. (B) Shrinkage.

3. Results and discussion

3.1. Water sorption isotherms

The water adsorption–desorption isotherms at 23 °C are shown (Fig. 2A–F). The shape of the different

isotherms obtained here seems to correspond to types II and III of the modern IUPAC classification of isotherms (Aranovich and Donohue, 1998). Type II describes the isotherms with high solid–fluid interaction. In contrast, type III describes the isotherms with small solid–fluid interaction. The Ca-saturated

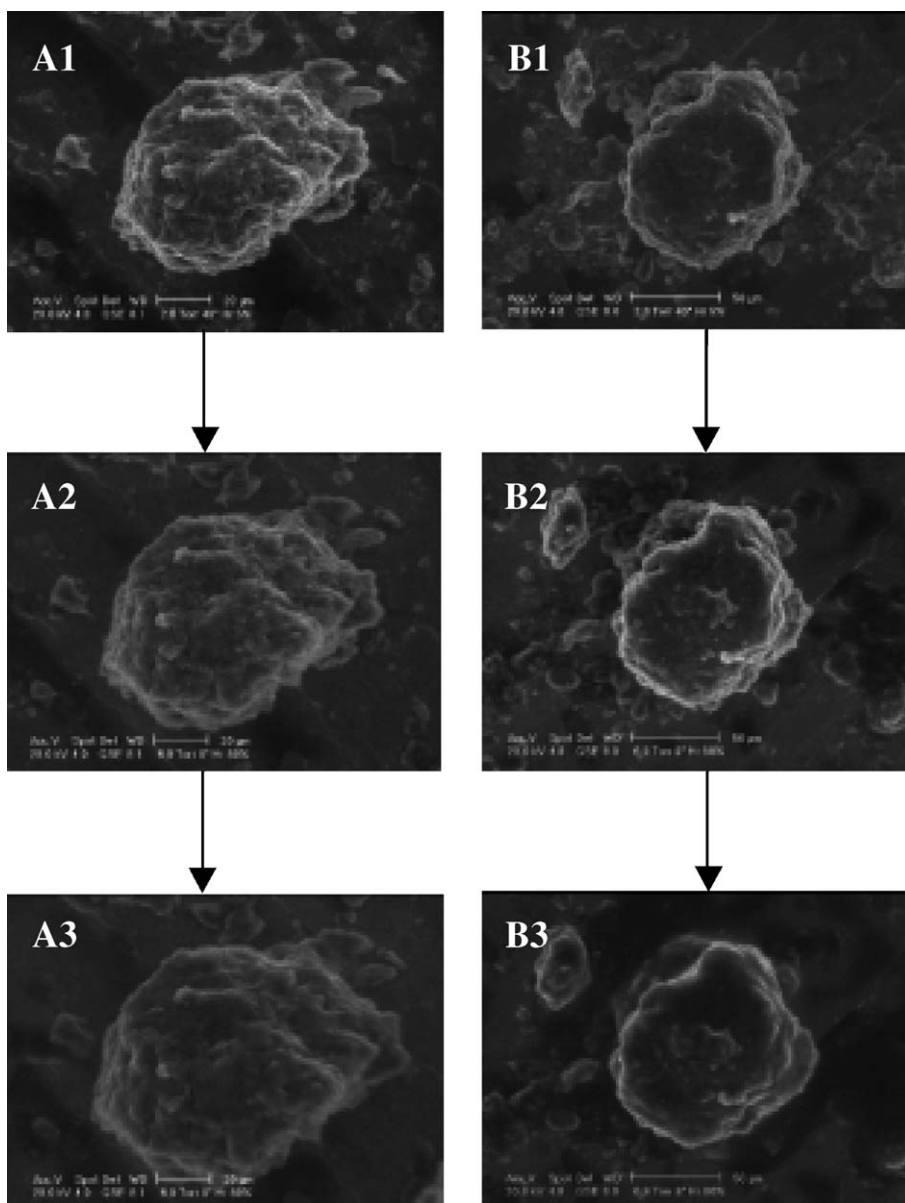


Fig. 4. Swelling comparisons of cation-saturated bentonites “ESEM analysis”. (A) Na-saturated bentonite. (B) Li-saturated bentonite. (1) initial state ($a_w=0.05$). (2) Hydrated state before water oversaturation ($a_w=0.8$). (3) Water oversaturation beginning ($a_w=0.8$).

and Mg-saturated bentonite shows a very high potential for water adsorption at low water activities (<0.5). This is typical of type II isotherms. In clay systems, this may correspond to the formation of water double layers around the divalent cations (Pons, 1980; Kraehenbuehl, 1987). The water adsorp-

tion at high water activities (>0.5) is also important (comprises capillary condensation), but lower than the amount of water sorption presented by Na-saturated and Li-saturated bentonite. The isotherms of “monovalent cations”-saturated bentonite (Li^+ , Na^+ , and K^+) show a small potential for water adsorption

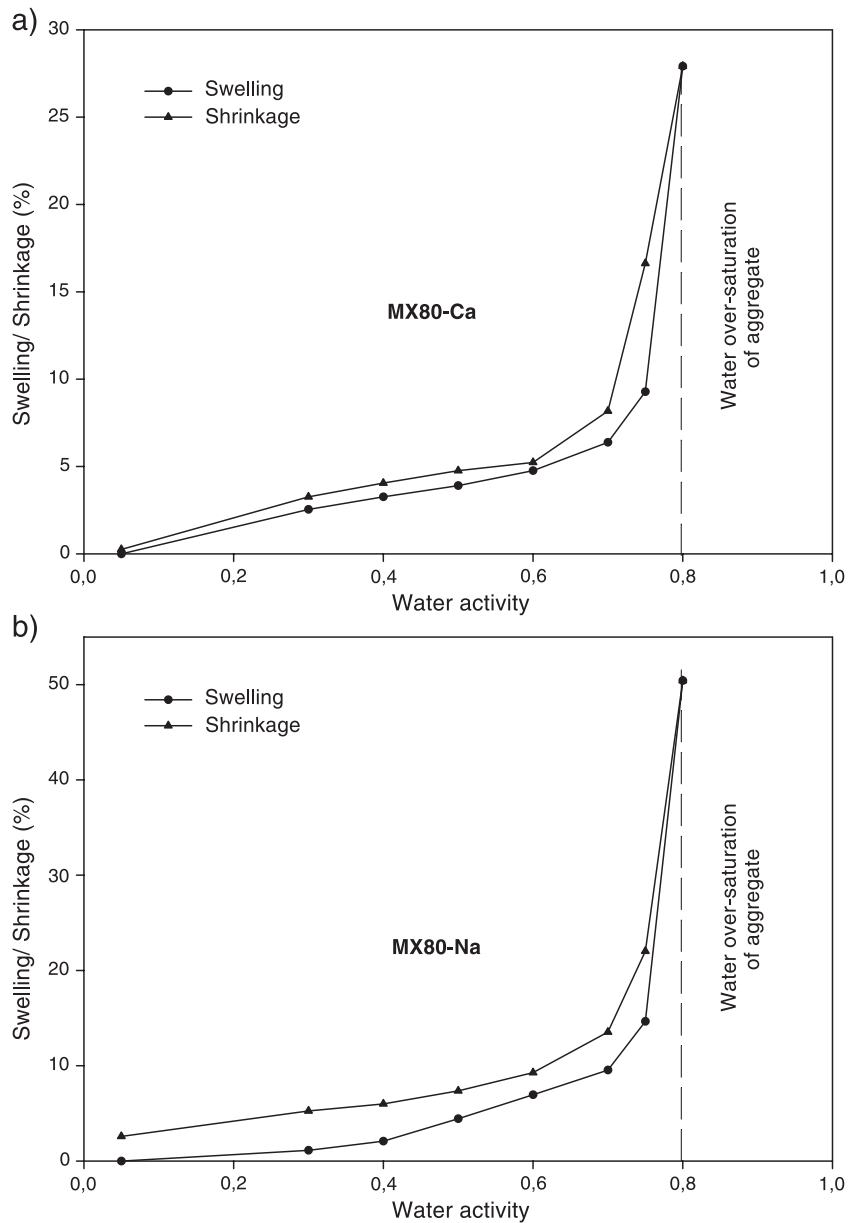


Fig. 5. Hysteresis phenomena between swelling and shrinkage. (a) Ca-saturated bentonite “MX80–Ca.” (b) Na-saturated bentonite “MX80–Na.”

at low water activities (<0.5). This is typical of type III isotherms. In contrast, the potential of water adsorption at high water activities (>0.5) is very high in particular for Na-saturated and Li-saturated bentonite. This may correspond to the formation of water multilayer around the cations and also to the water capillary condensation.

It is necessary to mention that isotherms types II and III in the IUPAC classification were proposed to describe macroporous systems. In general, that is not the case for clay minerals. In addition, the interlayer cations play an important role in water adsorption and swelling. This situation makes a complex mechanism for water adsorption as a function of water activity.

For all samples (i.e., raw bentonite and cation-saturated bentonite), the water adsorption–desorption isotherms present a hysteresis loop with the branches approximately parallel to one another (Fig. 2). All samples retain a certain amount of water at low water activity, which cannot be removed except by drying at room temperature. This indicates the existence of some highly hydrophilic adsorption sites (Sychev et al., 2001).

Finally, the absolute error (estimated by Eq. (2)) remains relatively low during water adsorption and/or desorption. The total error interval lies between 0.00015 and 0.00050 ($\text{g}_{\text{H}_2\text{O}}/\text{g}_{\text{dry clay}}$). This signifies that the maximum error represents only about 7% of the amount of adsorbed water in the worst case (i.e., at low water activity).

3.2. Swelling–shrinkage isotherms

The swelling–shrinkage isotherms at 9 °C are shown in Fig. 3A and B. Theoretically, the swelling–shrinkage potential in expansive clays is proportional to the potential of water sorption (i.e., when the amount of water sorption increases, the swelling–shrinkage potential also increases). This hypothesis does not strictly apply for the observations on Li-saturated bentonite; in fact, this sample presents a high potential for water adsorption (Fig. 2), but Fig. 3A and the ESEM analysis (Fig. 4) show that Li-saturated bentonite does not swell significantly at the aggregate scale. The explanation for this phenomenon may be due to the interlayer lithium cations that are irreversibly fixed in the octahedral cavities during sample drying (Tabikh et al., 1960 cited in Rico-Gamboa,

1984). The water sorption is then governed by the interparticle porosity and by the lithium cations fixed on the external surface.

On the other hand, the potential for water adsorption for the K-saturated bentonite remains low when it is compared with the other cation-saturated samples.

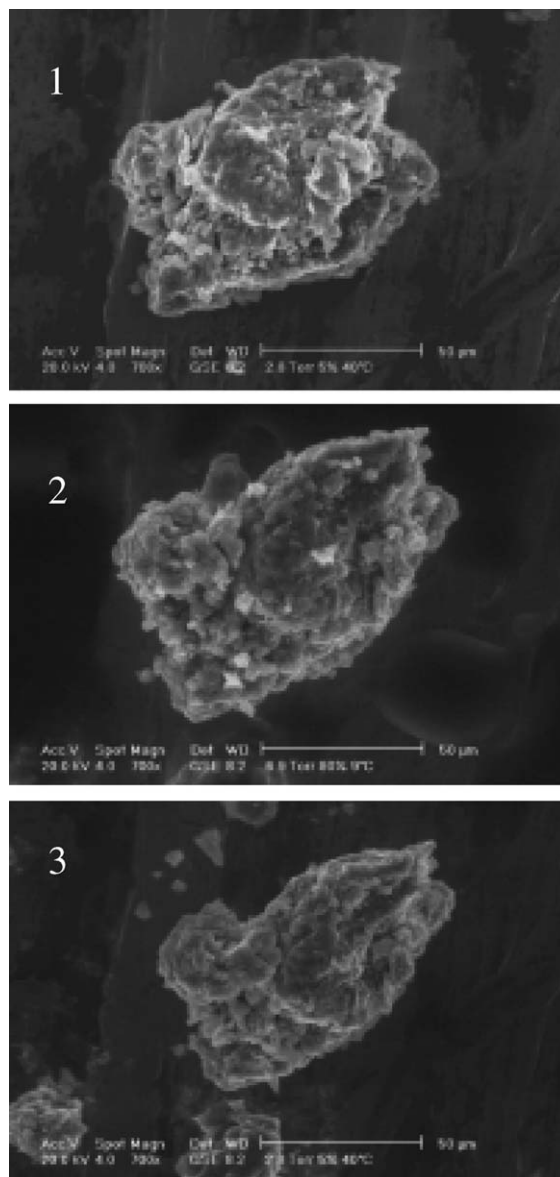


Fig. 6. Aggregate deformation after water oversaturation. Example of Mg-saturated bentonite. (1) Initial state ($a_w=0.05$). (2) Water oversaturation beginning ($a_w=0.8$). (3) After water oversaturation ($a_w=0.75$).

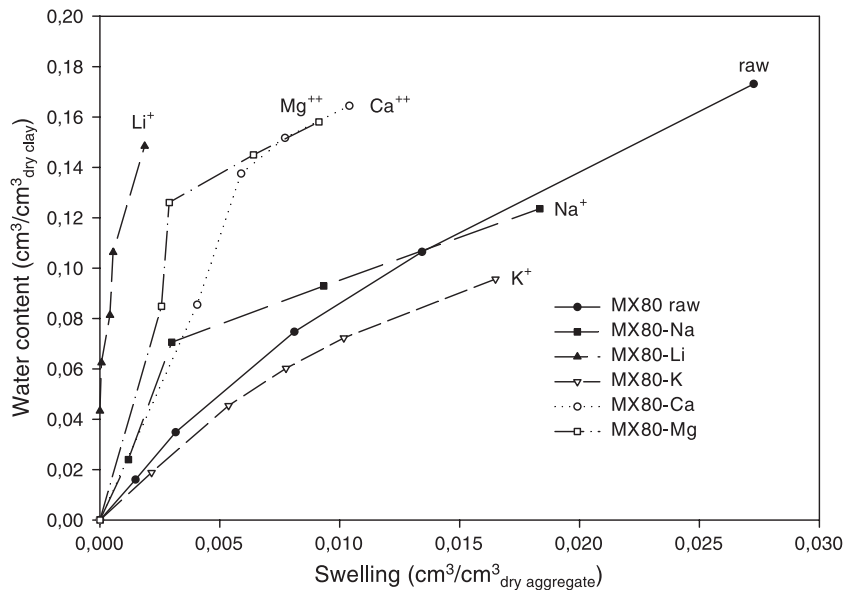


Fig. 7. Amount of adsorbed water and swelling potential correlation for natural and cation-saturated bentonite. Considerations: (1) adsorbed water in the sample was considered as an ideal gas; and (2) swelling potential was considered as equidimensional to aggregate scale.

In contrast, its swelling potential is significant. This phenomenon is normal since the natural bentonite presents a low interlayer charge ($\sigma \cong 0.3$), then the K-saturated bentonite behaves like an interstratified illite/smectite with the interlayer space of high charge closed at 10 Å (Mermut, 1994). This leads to a partial blocking of the swelling, affecting both water adsorption and swelling potential.

All swelling–shrinkage isotherms present a hysteresis phenomena similar to the water adsorption–desorption isotherms (see Fig. 5a and b). However, the experimental system “ESEM-DIA” used in the current work induces other causes of hysteresis (e.g.,

the irreversible deformation produced by water oversaturation in the aggregates) (Fig. 6).

In this case, the absolute error (estimated by Eq. (5)) on the swelling–shrinkage remains relatively low. Obviously, the error is more significant at low water activity or when the swelling–shrinkage is low.

3.3. Correlation between water adsorption and swelling

A Cartesian system was used to correlate the water adsorption and the swelling. This diagram shows a nonlinear correlation (Fig. 7). For this reason, a swelling-to-water sorption ratio was calculated for low, medium, and high water activity (0.3, 0.5, and 0.75, respectively) (Table 3). This basic approach must be considered with care since the measurements of the amount of adsorbed water and swelling potential were estimated separately by different analytical methods with different scales.

Table 3

The swelling-to-water sorption ratio for low, medium, and high water activity

Sample	Swelling-to-water adsorption ratio		
	Low ($a_w = 0.3$)	Medium ($a_w = 0.5$)	High ($a_w = 0.75$)
MX80 raw	0.0907	0.1085	0.1575
MX80–Na	0.0425	0.1005	0.1485
MX80–Li	0.0051	0.0052	0.0126
MX80–Ca	0.0428	0.0509	0.0633
MX80–Mg	0.0230	0.0442	0.0578
MX80–K	0.1182	0.1289	0.1725

4. Conclusion

Coupled ESEM-DIA is a powerful tool to observe and measure changes during swelling and shrinkage

of bentonite aggregates. Thus, the influence of interlayer cation on the swelling–shrinkage behavior was pointed out. The main advantage of this method is the speed with which one obtains the qualitative and quantitative results. However, this method allows only the ability to estimate the free swelling–shrinkage potential in the sample chamber.

The qualitative and quantitative comparison between the water adsorption and swelling isotherms shows that the amount of adsorbed water and the swelling potential of MX80 bentonite are governed by the nature of interlayer cation. For example, the Na-saturated bentonite presents an excellent capacity to adsorb water and to swell while the Li-saturated bentonite does not swell significantly at the aggregate scale; however, its water adsorption isotherm shows an excellent capacity to adsorb water. In addition, other textural properties may be modified by the cation saturation, such as the specific surface, the particle size, porosity, etc.

Acknowledgements

The authors are grateful to the National Council of Science and Technology, Mexico, and the Louis Pasteur University, France, for providing financial grants for this work.

References

- Aranovich, G., Donohue, M.D., 1998. Adsorption hysteresis in porous solids. *Journal of Colloid and Interface Science* 205, 121–130.
- Kraehenbuehl, F., 1987. Study of the water–bentonite system by vapour adsorption, immersion calorimetry and X ray techniques: I. Micropore volumes and internal surfaces areas, following Dubinin's theory. *Clay Minerals* 22, 1–9.
- Lee, S.Y., Kim, S.J., 2002. Delamination behaviour of silicate layer by adsorption of cationic surfactants. *Journal of Colloid and Interface Science* 248, 231–238.
- Luckham, P.F., Rossi, S., 1999. The colloidal and rheological properties of bentonite suspensions. *Advances in Colloid and Interface Science* 82, 43–92.
- Mermut, A.R., 1994. Layer charge characteristics of 2:1 silicate clay mineral. *Clay Minerals Society Workshop Lectures* 6, 134 pp.
- Montes-H, G., 2002. Etude expérimentale de la sorption d'eau et du gonflement des argiles par microscopie électronique à balayage environnementale (ESEM) et analyse digitale d'images. PhD Thesis. Louis Pasteur University, Strasbourg I, France.
- Newman, A.C.D., 1987. Chemistry of clays and clay minerals. Monograph No. 6, Mineralogical Society. 480 pp.
- Pons, C.-H., 1980. Mise en Evidence des Relations entre la Texture et la Structure dans les Systèmes EAU-SMECTITES par Diffusion aux Petits Angles du Rayonnement X Synchrotron. PhD Thesis. Orleans University, France. 175 pp.
- Rico-Gamboa, 1984. Thermodynamique de l'échange cationique dans les argiles. PhD Thesis. Louis Pasteur University, Strasbourg I, France. 154 pp.
- Rousset-Tourmier, B., 2001. Transferts par capillarité et évaporation dans des roches—rôle des structures de porosité. PhD Thesis. Louis Pasteur University, Strasbourg I, France. 204 pp.
- Rytwo, G., 1996. Exchange reactions in the Ca–Mg–Na–Montmorillonite system. *Clays and Clay Minerals* 44 (2), 276–285.
- Sychev, M., Prohod'ko, R., Stepanenko, A., Rozwadowski, M., de Beer, V.H.J., Van Sarten, R.A., 2001. Characterization of the microporosity of chromia- and titania-pillared montmorillonites differing in pillar density: II. Adsorption of benzene and water. *Microporous and Mesoporous Materials* 47, 311–321.
- Touret, O., 1988. Structures des Argiles Hydratées, Thermodynamique de la Déshydratation et de la Compaction des Smectites. PhD Thesis. Louis Pasteur University, Strasbourg, France. 172 pp.
- Velde, B., 1992. Introduction to Clay Minerals: Chemistry, Origins, Uses and Environmental Significance, 1st ed. Chapman and Hall. 195 pp.